Effect Of Initial Stress Anisotropy On The Cyclic Behaviour Of Sand

Dr. Mohammed Yousif Fattah*

Received On: 4/ 7 / 2004
Accepted On: 26 / 6 / 2005

Abstract

Due mainly to the process of deposition under earth gravity, the behavior of in situ sand is inherently anisotropic, meaning the stress-strain-strength relations for the same sand may vary as the stress tensor rotates relative to the orientation of the soil fabric.

In this paper, the kinematic double hardening model ALTERNAT is applied to simulate the cyclic behaviour of sand. The model can describe several phenomena of sand behaviour such as the stress dilatancy, hardening, densification and cyclic mobility. The effect of initial stress anisotropy through the values of the coefficient of lateral stress at rest (Ko) is studied.

It is concluded that the maximum shear strain increases with the increase of the coefficient of lateral stress at rest. On the other hand, the maximum spherical (volumetric) strain decreases with the increase of the coefficient of lateral stress at rest until a value of about (Ko=0.72) is reached, above this value, the maximum spherical strain increases. This behaviour reflects the stress dilatancy that takes place in dense sand where the values of Ko are high. The stress dilatancy increases as the value of Ko increases at the start of loading. As the number of increments increases, the effect of Ko decreases. This can be attributed to the densification that might take place under cyclic loading till the sand reaches a stable condition.

Keywords:Alternat model, Stress Anisotropy, Dilatancy, Hardening

تأثير عدم تماثل الإجهاد الأولي على السلوك الدوري للرمل

الخلاصة

إن سلوك الرمل موقعيا يعتبر سلوكا غير متماثل ضمنيا لأسباب أهمها يعود إلى عملية الترسيب تحت تأثير الجاذبية الأرضية. إن عدم التماثل يعني أن علاقات

* Lecturer, Building and Construction Eng. Department, University of Technology.

https://doi.org/10.30684/etj.24.5.2
University of Technology-Iraq, Baghdad, Iraq/2412-0758

الإجهاد-الانفعال لنفس الرمل قد تتغير مع تدوير مشبك الإجهاد نسبة إلى تدوير بنية الرمل.

في هذا البحث طبق النموذج ثنائي التصلب المسمى (ALTERNAT) في تمثيل السلوك الدوري للرمل. هذا النموذج له القابلية على وصف ظواهر عديدة للرمل مثل التمدد بالإجهاد و التصلب و التكثيف و الانتقال الدوري. و قد درس تأثير عدم تماثل الإجهاد الأولي من خلال قيم معامل الإجهاد الجانبي في حالة السكون (Ko).

و قد توصل البحث إلى أن انفعال القص الأقصى يتزايد مع زيادة معامل الإجهاد الجانبي في حالة السكون. و من ناحية أخرى، يتناقص الانفعال الحجمي الأقصى مع زيادة قيم (Ko) وصولا إلى قيمة تساوي تقريبا (Ko=0.72)، و بعد هذه القيمة يتناقص الانفعال الحجمي الأقصى. ان هذا السلوك يعكس تأثيرات التمدد بالاجهاد التي قد تحدث في الرمل الكثيف حيث تكون قيم (Ko) عالية. و يتزايد التمدد بالإجهاد مع زيادة قيم (Ko) في بداية التحميل. و مع زيادة عدد التحميلات يتناقص تأثير (Ko)، و هذا يمكن أن يعزى إلى التكثيف الذي يمكن أن يحدث تحت تأثير الأحمال المتكررة حتى يصل الرمل الى حالة الاستقرار.

1. Introduction:

Subjected to shear, loose sand contracts and dense sand dilates. Whether sand is in a loose or dense state depends not only on the density of the sand but also on the confining pressure applied. Furthermore, for a sand that initially is in either a loose or a dense state, there is an ultimate state of shear failure at which the volumetric strain rate is zero. This ultimate state is the well-known steady or critical state. Li and Dafalias (2000) pointed out that the classical stress dilatancy theory (Rowe, 1962) in its exact form ignored the extra energy loss due to the static and kinematical constraints at particle contacts and led to a unique relationship between the stress ratio and dilatancy. It has been shown (Li and Dafalias, 2000) that, in order to model sand behavior over a full range of density states, additional dependence of dilatancy on the material internal state is needed, and the material state must be described in reference to the critical/steady state line in the *e-p-q* space.

In addition, due mainly to the process of deposition under earth gravity, the behavior of in situ sand is inherently anisotropic, meaning the stress-strain-strength relations for the same sand may vary as the stress tensor rotates relative to the orientation of the soil

fabric. Experimental investigations in the past 15 years on flow liquefaction of earth structures have revealed that the influence of inherent fabric anisotropy on the residual strength of a granular soil is so drastic that the inherent anisotropy can no longer be ignored in sand modeling.

However, due primarily to insufficient understanding of the physical mechanisms and to the complexity of the underlying mathematical theories, the issue is in general not rigorously treated in current modeling practice. In fact, for simplicity, quite a number of existing sand models either totally ignore the influence of inherent fabric anisotropy or simply introduce biased parameters to different orientations without satisfying basic objectivity requirements. These models are somewhat far-fetched when the influence of fabric anisotropy is significant and the loading conditions are complex, (Li, 2002).

2. Importance of Anisotropy in Sand:

Undrained cyclic triaxial test has been widely performed for evaluating liquefaction phenomena in sandy deposit. In cyclic triaxial test, the 45° inclined plane in the specimen represents the shear plane (typically the horizontal plane) in the ground, and the cyclic shear stress (i.e. the half of the deviator stress) on the 45° inclined plane simulates the cyclic loading during earthquake. This assumption is reasonable if the soil is isotropic in mechanical behavior. However, many researchers recently reported strong anisotropic nature of sandy materials in undrained shear (Nakata et al., 1998 and Yoshimine et al., 1998). Figure (1) shows the result of undrained triaxial compression and extension tests in monotonic loading (test data from Yoshimine et al., 1998). The stress path indicates that the triaxial extension loading exhibited much more compressive behavior and resulted in much smaller strength compared with the test result from triaxial compression loading. Such prominent anisotropic nature may also affect the undrained behavior of the material during cyclic triaxial loading test, especially when initial shear stress is applied to the triaxial specimen before undrained cyclic loading.

In the monotonic loading tests, it was found that the undrained

behavior was seriously affected by the anisotropic nature of the sand deposit. Triaxial extension exhibited much softer behavior compared with triaxial compression. The effect of initial shear on the undrained monotonic loading was minor than that of the shear direction, though slight increase of shear resistance was observed when initial shear stress level was higher, (Yoshimine, 2002).

3. Modeling of Inherent Anisotropy:

Vaid and Chern (1985) were among the first to show, through undrained triaxial tests, that the critical state strength of sand measured in extension was much lower than that in triaxial compression under otherwise identical conditions, and that the significant difference was directly associated with the soil dilatancy. Investigations at the microscopic level have shown that even after a very large macroscopic shear deformation, the preferred orientation of the particles in a granular material has only undergone a limited change. In other words, the inherent fabric anisotropy of the sand may well endure after the onset of the critical state. Nakata et al. (1998) performed a series of hollow cylinder undrained torsional tests that allowed to control the directions of principal stresses in reference to the direction of soil deposition, as measured by the angle α shown in Figure (2), and the ratios between the principal stresses as measured by $b = (\sigma_2 - \sigma_3)/(\sigma_1 - \sigma 3)$. The test results confirmed that the sand responses, and in particular the sand dilatancy and the stress paths towards critical state failure, were indeed significantly affected by the directions of the principal stresses relative to the orientation of soil specimen. This means that the inherent fabric anisotropy of a granular soil could have a significant impact on the dilatancy and the critical state failure of the soil.

In this paper, the ALTERNAT model will be applied to model the effect of initial stress anisotropy on the cyclic behaviour of sand.

4. The ALTERNAT Model:

The ALTERNAT model described in this paper forms the major component of a double hardening model for the mechanical behaviour of sand under alternating loading.

The model was developed by Molenkamp (1987) at Delft Geotechnics. In Figure (3), the yield surfaces of both plastic models, namely the

"compressive" model and the "deviatoric" model are shown in the stress space of the isotropic stress, s, and the deviatoric stress, t.

The kinematic rule relates the change of the anisotropy to the change of the stress. It is based on the assumption that the boundary between the elastic and elasto-plastic subspaces does not change during continued loading after a stress reversal. The volume change as described by the model is based on the dilatancy theory (Rowe, 1962 and 1971) in which the effect of load history does not occur.

For monotonic and alternating loading, the hardening modulus is assumed to depend on two load history effects. One effect concerns the stress-induced anisotropy. It is described by the distribution of the kinematic hardening modulus in stress space, which depends on the distribution of the kinematic yield surfaces in stress space. The other effect involves the effect of the densification due to alternating loading. It is described by the so-called load history function, K. Through this function, the hardening modulus becomes also dependent on the initial density and the instantaneous density, (Molenkamp, 1987).

4.1 Definition of Kinematic Plastic Model and Kinematic Rule:

Using the elastic and plastic strains and the stress Σ together with their rates, the constitutive models in the current state can be defined on the cartesian co-rotational base vectors, γ_i.

The elastic model will be of the form, (Molenkamp, 1987):

$$\varepsilon_{ij}^{e} = function(\Sigma_{kl}) \quad \text{.... (1)}$$

The irreversible Eulerian strain rates or increments, $\dot{K}_{ij}$, are described by a plastic kinematic hardening model of the form, (1987):

$$\dot{K}_{ij} = \frac{\frac{\partial G}{\partial \Sigma_{ij}} \frac{\partial F}{\partial \Sigma_{kl}} \Sigma_{kl}^{o}}{H} \quad \text{.... (2)}$$

in which: $F(T_{ij}, \chi) = 0$: yield surface.

$G(T_{ij}, \chi_1) = 0$: plastic potential.

$H(T_{ij}, \xi_{kl}, w_{mn}, \chi)$: hardening.

$T_{ij} = \Sigma_{ij} - \zeta_{ij}$: pseudo stress .... (3)

w : plastic deformation.

ξ_{ij} : tensor of anisotropy representing the effect of the anisotropic fabric.

χ : quantity describing the size of the kinematic yield surface; the so- called hardening parameter.

χ_l : idem for plastic potential.

Figure (4) illustrates the above conditions.

In the description of this motion, the following stresses are relevant:-

Σ : stress at last stress reversal,

Σ_n : stress at the beginning of a new stress increment,

Σ_{new} : stress at the end of a new stress increment,

Besides, the following tensors of anisotropy are relevant.

ξ : tensor of anisotropy of the yield surface which was just activated before the last stress reversal,

ξ_n : tensor of anisotropy of the yield surface which was just activated by the stress at the beginning of the new stress increment, and

ξ_{new} : tensor of anisotropy of the new yield surface at the end of the new stress increment.

Finally, the following hardening parameters play a role:

χ : hardening parameter of the yield surface just before the stress reversal, and

χ_n, χ_{new}: hardening parameters of the yield surface at the start and end of the increment, respectively.

The problem is how to find ξ_{new} and χ_{new} while Σ_{new} is known. The first condition of the motion of the new kinematic yield surface describes that both the new yield surface (with ζ_{new}) and the yield surface at stress reversal (with ζ) have to be tangent to each other at the stress point of stress reversal, Σ, (Lade, 1979), thus:

$$C \frac{\partial F}{\partial \Sigma_{ij}} (\Sigma, \xi, \chi) = \frac{\partial F}{\partial \Sigma_{ij}} (\Sigma, \xi_{new}, \chi_{new}) \quad \ldots (4)$$

for some constant C. The derivation of the above equation is reported by Fattah (1999).

4.2 The Yield Surface For The Deviatoric Model:

For the continuum model of a uniform stack of rigid discs, a kind of kinematic yield surfaces was found, in which the relevant measure of stress appeared to be a shear stress level (Molenkamp, 1980). For the present kinematic model, a similar measure of relevant stress is introduced, namely the shear stress level which is defined by:

$$\frac{t_{ij}}{\frac{I_1}{3}} = \frac{\sigma_{ij} - \frac{I_1}{3}\delta_{ij}}{\frac{I_1}{3}} \quad \ldots\ldots (5)$$

in which: t_{ij} = deviatoric stress.

$I_1 = \sigma_{ij}\ \delta_{ij}$ = first stress invariant.

This relevant measure of stress is dimensionless.

For the tensor of anisotropy, also a dimensionless deviatoric tensor, ξ, is introduced, thus $\xi_{ij}\ \xi_{ij} = 0$. The relevant measure of the pseudo shear stress level becomes:

$$\frac{X_{ij}}{\frac{I_1}{3}} = \frac{t_{ij}}{\frac{I_1}{3}} - \xi_{ij} \quad \ldots\ldots (6)$$

in which: X_{ij} = deviatoric pseudo stress tensor.

Substituting Equation (6) in (5) leads to the pseudo stress tensor, T_{ij}, being defined as follows:

$$T_{ij} = X_{ij} + \delta_{ij}\ \frac{I_1}{3} = \sigma_{ij} - \xi_{ij}\ \frac{I_1}{3} \quad \ldots. (7)$$

The yield surface for the deviatoric model is of the form:

$$F^d = F^d(I_1, I_2, I_3, \chi) = 0 \quad \ldots. (8)$$

in which I_1, I_2 and I_3 are three invariants of the pseudo stress T_{ij},.

The expression chosen for the yield surface F^d should reduce to a generally accepted expression for monotonic loading when $\xi_{ij} = 0$. The expression as introduced by Lade and Duncan (1975) is used:

$$F^d = \frac{I_1^3}{I_3} - 27 - f^d(\chi) = 0 \quad \ldots. (9)$$

in which:

$$f^d = \frac{I_1^3}{I_3} - 27$$

measure of the shear stress level, constant at a kinematic yield surface.

4.3 The Plastic Potential for the Deviatoric Model:

In a plastic material model, the plastic potential describes the ratio of the Eulerian strain rates. For simplicity, it is assumed that the ratios of the plastic Eulerian strain rates can be described in the following way:

$$\varepsilon_y^d = \left\{ \alpha\xi_{ij} + \frac{\partial G^{dd}}{\partial \sigma_{ij}} \right\} = \lambda \frac{\partial G^d}{\partial \sigma_{ij}} \quad \ldots. (10)$$

in which:

$$\frac{\partial G^{dd}}{\partial \sigma_{ij}}\ \xi_{ij} = 0 \quad \ldots (11)$$

deviatoric tensor and

$$\frac{\partial G^{dd}}{\partial \sigma_{kl}} \frac{\partial G^{dd}}{\partial \sigma_{kl}} = 1 \quad (12)$$

α is the ***angle of noncoaxiality*** which is the angle between the principal directions of stress and the Eulerian strain rates.

Like the yield surface, the deviatoric component of the plastic potential G^{dd} is based on the failure surface of Lade and Duncan (1975), namely:

$$F^* = \frac{I_1^{3^*}}{I_3^*} - 27 - f^{d^*} = 0 \quad \ldots. (13)$$

in which: I^*_1 , I^*_3 are the first and third invariants of the pseudo stress T^*_{ij}. The pseudo stress T^*_{ij} has the same isotropic component as the pseudo stress $T_{ij} = \sigma_{ij} - I_1/3$ as used for the yield surface but a smaller deviatoric part, namely:

$$T^*_{ij} = \sigma^*_{ij} - \frac{I_1}{3}\xi_{ij} = \frac{I_1}{3}\delta_{ij} + RT^*(\sigma_{ij} - \frac{I_1}{3}\delta_{ij} - \frac{I_1}{3}\xi_{ij})$$

$$T^*_{ij} = \frac{I_1}{3}\delta_{ij} + RT^*(T_{ij} - \frac{I_1}{3}\delta_{ij}) \quad (14)$$

thus:

$$\sigma^*_{ij} = (1 - RT)(\delta_{ij} - \xi_{ij})\frac{I_1}{3} + RT\sigma_{ij} \quad (15)$$

where RT is a material constant.

Thus to each pseudo stress, T_{ij} of the yield surface, another pseudo stress, T^*_{ij} is concerned using the same tensor of anisotropy ξ_{ij} $I_1/3$, and the same isotropic component but a smaller deviatoric component as shown in Figure (5).

4.4 Stress Dilatancy:

Molenkamp (1980) elaborated the stress dilatancy theory for triaxial compression and triaxial extension tests. For loading towards failure in triaxial compression, it was found that:

$$\frac{\dot{V}}{\dot{\gamma}} = \frac{-\sqrt{2}(1-K) - (2+k)\frac{t}{s}}{(1+2K) + \sqrt{2}(1-K)\frac{t}{s}} \quad \ldots. (16)$$

in which:

$$K = \tan^2(45 + \frac{\phi_o}{2})$$

V = volumetric strain, and

γ = deviatoric strain

and ϕ_o is the interparticle friction angle. It is assumed that, (Molenkamp, 1980):

$$\phi_o = \phi_{cv} - (\phi_{cv} - \phi_\mu) \exp\left(\frac{-s}{Pa.S_{cv}}\right) \quad \ldots(17)$$

in which:

ϕ_μ = interparticle friction angle at very low isotropic stress s,

ϕ_{cv} = interparticle friction angle at very high isotropic stress,

S_{cv} = parameter describing the rate by wich ϕ_o changes from ϕ_μ to ϕ_{cv} with increasing isotropic stress level (s/Pa), (see Figure 6), and

Pa = atmospheric pressure.

For loading towards failure in triaxial extension, it was found that:

$$\frac{\dot{V}}{\dot{\gamma}} = \frac{\sqrt{2}(1-K) - (1+2K)\frac{t}{s}}{(2+K) - \sqrt{2}(1-K)\frac{t}{s}} \quad \ldots (18)$$

In order to distinguish between loading and unloading, the following quantity is defined:

$$\frac{\partial G^{dd}}{\partial \sigma_{ij}} \frac{t_{ij}}{\sqrt{t_{kl}t_{kl}}} \quad \ldots (19a)$$

The quantity of Equation (19a) can vary between +1 and -1. Loading is defined by:

$$0 < \frac{\partial G^{dd}}{\partial \sigma_{ij}} \frac{t_{ij}}{\sqrt{t_{kl}t_{kl}}} < 1 \quad \ldots. (19b)$$

and unloading occurs if the quantity is between 0 and -1.

During failure, the deviatoric stress does not change anymore, while the shear strain keeps increasing. At the critical state, the volume change stops. This is illustrated in Figure (7).

4.5 Stress Induced Anisotropy Described by the Kinematic Hardening:

For simplicity, the functional form of the kinematic hardening H_{kin} is chosen as follows:

$$H_{Kin} = H_{Kin}(I_T, \chi) \quad (20)$$

in which:

I_T = invariants of the pseudo stress T_{ij}.

The kinematic hardening H_{kin} can be calculated from experimental data as follows:

$$H_{Kin} = \frac{\frac{\partial F^d}{\partial \sigma_{kl}} \sigma^o_{kl}}{K * \dot{\gamma}^d} = \frac{\frac{\partial F^d}{\partial \sigma_{kl}} \sigma^o_{kl}}{\dot{\gamma}_{Kin}} \quad \ldots (21)$$

The curve of the shear stress level $(t/s)_c$ in drained triaxial compression at an isotropic pressure (s/Pa) = 1 is related to the deviatoric strain (see Figure 8) by, (Molenkamp, 1985):

$$\left(\frac{t}{s}\right)_c = \frac{Y_1 \; Y_2}{(Y_1^n + Y_2^n)^{(\frac{1}{n})}}$$

... (22)

in which:

n = quantity larger that 1.

Y_1, Y_2 = two approximations of the shear stress level versus plastic deviatoric strain curve of drained triaxial compression at s = Pa.

Details of the functions Y1 and Y2 are given by Molenkamp (1987) and Fattah (1999).

4.6 Effect of Densification Described by the Load History Function:

The load history function describes the effects of densification due to cyclic preloading. With increasing number of cycles and related densification, the load history function, K, will also increase.

It is assumed that this component of the hardening can be related to the instantaneous density at the last stress reversal. The expression for K should become infinite at maximum densification, because in such a case, neither plastic densification nor plastic shear strains will occur and the hardening H^d of the present plastic model will be infinite.

4.7 Kinematic Rule for The Deviatoric Model:

The kinematic rule, as applied in ALTERNAT model, is based on the assumption that the kinematic yield surfaces remain tangent to each other at the stress reversal points.

In order to illustrate the structure of the kinematics of the model, the motion of the yield surfaces during alternating loading is described for several phases of loading, unloading and reloading. Initially, it is assumed that the principal directions of stress coincide with the co-rotational base vectors and that the material is isotropic initially. If in the initial state, the material is isotropic, then the yield surfaces in the pi-plane will be centered on the isotropic axis (see Figure 9a).

During initial loading from some isotropic state as shown in Figure (9b) to some shear stress level (point 2), all the yield surfaces with lower hardening parameter, $f^d(\chi)$, than point 2 are displaced and they are passing through point 2 while being tangent to the isotropic yield surface through point 2.

During unloading from point 2 towards for instance point 3 as shown in Figure (9c), the total behaviour is initially elastic, because at low hardening parameters $f^d(\chi)$, the present deviatoric model is completely rigid. All yield surfaces with a lower hardening

parameter $f^d(\chi)$ than the yield surface passing through both points 2 and 3 are displaced during this change and they are passing through point 3 while being tangent to the yield surfaces passing through both points 2 and 3.
During reloading from point 3 to point 4 and further, (see Figure 9d), similar stages are passed through like the case of unloading from point 2 to point 3, thus the initial total elastic behaviour is followed by an increasing rate of plastic deformation further on.

If during further loading, the lowest isotropic yield surface (through point 2) is passed as for instance during loading from point 4 up to point 5 as shown in Figures (9d and e), then all the yield surfaces with lower hardening parameter $f^d(\chi)$ than the isotropic yield surface through point 5 are displaced and are passing through point 5 while being tangent to this isotropic yield surface. It should be noted that the same situation would have been obtained if point 5 had been reached directly by loading from the isotropic state.

A parameter called "**anisot**" is introduced describing whether the inner region of the relevant yield surface with hardening parameter χ_K and tensor of anisotropy ξ_K consists of:
a) anisotropic yield surfaces, then anisot = 1.
b) isotropic yield surfaces, then anisot = 0. In this exceptional case, all smaller kinematic yield surfaces have ξ_K as tensor of anisotropy, the current stress may be inside the yield surface f^d_K.

Molenkamp (1987) described different possible loading conditions, some of which are:

1. Loading starting at a stress situated on the outermost isotropic yield surface.
2. Loading starting at a stress inside the outermost yield surface and leading to a new stress situated on the outermost isotropic yield surface.
3. Loading starting at a stress inside the outermost yield surface and leading to a new stress situated inside the outermost yield surface.

4.8 Decision on The Type of Behaviour:

The stress increment $d\sigma_{kl}$ due to a strain increment $d\varepsilon_{ij}$ is given by the elasticity matrix, D_{klij}, (Molenkamp, 1987):

$$d\sigma^e_{kl} = D_{klij} d\varepsilon_{ij} \qquad (23)$$

The quantity that determines whether this increment leads out of the current yield surface,

F = 0 is defined by, (Molenkamp, 1987):

$$dF^e = \frac{\partial F}{\partial \sigma_{kl}} d\sigma^e_{kl} \quad (24)$$

$dF^e > 0$ indicates an increment leading outside the current yield surface.

In case of elasto-plastic behaviour, the strain increment is given by:

$$d\varepsilon_{ij} = D^{-1}_{ijkl} d\sigma^{ep}_{kl} + \frac{\partial G}{\partial \sigma_{ij}} \frac{\frac{\partial F}{\partial \sigma_{kl}} d\sigma^{ep}_{kl}}{H} \quad \ldots\ldots \quad (25)$$

The quantity

$$dF^{ep} = \frac{\partial F}{\partial \sigma_{kl}} d\sigma^{ep}_{kl} \quad (26)$$

describes the direction of the stress increment with respect to the current yield surface. The elastic and elasto-plastic behaviour can be defined by:

$dF^{ep} > 0 \;, H > 0$ ***hardening***

$dF^{ep} < 0 \;, H < 0$ ***softening***

for elasto-plastic behaviour.

$dF^e < 0$ for elastic behaviour.

5. Definition of the Initial State:

In the definition of the initial state, the effect of the load history has to be accounted for. In the common case of a horizontal layer with only monotonic and uniform loading after sedimentation, the initial state can be described by three characteristic yield surfaces as shown in Figure (10) in which T_1, T_2 and T_3 are the principal stresses. The larger yield surface can be defined by the hardening parameter χ_1, thus $f^d_1 = f^d_1(\chi_1)$. Then the equivalent shear stress level $(t/s)_e$ in triaxial compression and the equivalent stress $\sum_1$ can be calculated.

The second characteristic yield surface f^d_2 is determined by assuming that in the initial state, the effective horizontal stress, $\sigma_{h'}$, is related to the effective vertical stress, $\sigma_{v'}$, by K_o (the coefficient of lateral stress at rest). In Figure (10), this point is indicated by the stress point $\sum_3$.

The computer program (INISTAT) has been written in FORTRAN – 77 Language depending on the subprograms given by Molenkamp (1987) and other subprograms. The program has the capability of defining the initial state and giving the points required to plot the characteristic yield surfaces. The parameters of the double hardening elasto-plastic kinematic hardening model ALTERNAT have been collected by Molenkamp (1987) and are also rearranged by Fattah (1999). In Figure (11),

the position of the relevant yield surfaces are shown in the pi-plane at an isotropic stress s =1 for different values of K_o. The effect of different initial states of anisotropy are considered. These initial states of anisotropy are described by the magnitude of K_o.

6. Zero-Dilatancy Rule:

Dilatancy is independent of the increment of stress or its direction for a fixed stress point, and can be approximated by a linear function of stress ratio, (Zienkiewicz et al., 1987):

$$dg = \frac{\dot{V}}{\dot{\gamma}} = (1+\alpha_g)(M_g - \eta) \quad \text{.... (27)}$$

where: $\eta = t/s$ and α_g is constant.

This simple rule predicts zero dilatancy whenever the line:

$$\eta = M_g \quad \text{.... (28)}$$

is reached.

Generalization to three-dimensional stress conditions can be done if a law of a Mohr-Coulomb type is assumed (Zienkiewicz and Pande, 1977) for the zero dilatancy line, giving (Zienkiewicz et al., 1987)

$$M_g = 6\sin\phi_g' / (3 - \sin\phi_g' \sin 3\theta) \quad \text{... (29)}$$

where θ is Lode's angle defined by Molenkamp (1987) as:

$$\sin 3\theta = 3\sqrt{6}\frac{J_{3_{\pi ij}}}{t^3}, \quad \frac{-\pi}{6} < \theta < \frac{\pi}{6} \quad \text{... (30)}$$

where: ϕ'_g = a constant residual angle of friction.

J_3 = the third invariant of the deviatoric pseudo stress tensor.

The computer program (STRESCON) was written in order to verify the capability of the ALTERNAT model in simulating cyclic loading. The description of this program and its subroutines was given by Molenkamp (1987) and Fattah (1999). The stress path that was considered is given in Figure (12). The plot of the shear stress level t/s versus isotropic stress s of this stress path is depicted in Figure (13).

The zero dilatancy rule had often been referred to as the "*critical state line*", "*characteristic state line*" or "*line of phase transformation*", a term coined by Ishihara et al. (1975). The zero dilatancy lines are illustrated in Figure (13).

The addition of the above definition of the zero-dilatancy line is a modification on the ALTERNAT model made by the author.

The numerical results for the strains are shown in Figures (14), (15) and (16). Several cases were considered in which the values of K_o were varied and some of the results are presented here. A comparison between Figures (15c) and (16c) shows that the stress dilatancy increases as the value of K_o increases at the start of loading. As the number of increments increases, the effect of K_o decreases. This can be attributed to the densification that might take place under cyclic loading till the sand reaches a stable condition.

It is noticed from Figures (14a), (15a) and (16a) that the shear strain increases for a given value of t/s as the value of K_o increases.

The initial condition of Figure (10b) depicts K_o-stress situation for $K_o = 0.7$. From this state, the deviatoric stress is decreased till it has a zero value.

In Figures (17), (18) and (19), the effect of the initial stress anisotropy through the coefficient of lateral stress at rest on both the invariant Y, the maximum shear strain and the spherical (volumetric) strain is presented.

It can be concluded that the maximum shear strain increases with the increase of the coefficient of lateral stress at rest. On the other hand, the maximum spherical strain decreases with the increase of the coefficient of lateral stress at rest until a value of about (K_o=0.72), above this value, the spherical strain increases. This behaviour reflects the stress dilatancy that takes place in dense sand where the values of K_o are high.

Conclusions:

In this paper, the kinematic double hardening model **ALTERNAT** is applied to simulate the cyclic behaviour of sand. The effect of initial stress anisotropy through the values of the coefficient of lateral stress at rest is studied. The followin conclusions can be obtained:

1. Different values of the coefficient of lateral stress at rest K_o revealed different positions of the relevant yield surfaces shown in pi-plane at an isotropic stress s = 1. This reflects the effect of different initial states of stress anisotropy which is described by the magnitude of K_o in this paper.
2. The stress dilatancy increases as the value of K_o increases at the start of loading. As the number of increments increases, the effect of K_o

decreases. This can be attributed to the densification that might take place under cyclic loading till the sand reaches a stable condition.

3. The maximum shear strain increases with the increase of the coefficient of lateral stress at rest. On the other hand, the maximum spherical (volumetric) strain decreases with the increase of the coefficient of lateral stress at rest until a value of about (K_o=0.72) is reached, above this value, the maximum spherical strain increases. This behaviour reflects the stress dilatancy that takes place in dense sand where the values of K_o are high.

REFERENCES:

1. Fattah, Mohammed Y., (1999). (The Non-Linear Dynamic Behaviour of Soils), Ph.D dissertation, University of Baghdad.
2. Ishihara, K., Tatsuoka, F. and Yasuda, S., (1975). (Undrained Deformation and Liquefaction of Sand Under Cyclic Stress), Soils and Foundations, JSSMFE, Japan, Vol. 15, No.1, p. p. 29 - 44.
3. Lade, P. V. and Duncan, J. M., (1975). (Elasto-Plastic Stress-Strain Theory for Cohesionless Soil), Journal of Geotechnical Engineering Division, ASCE, Vol. 101, GT10, p. p. 1037 - 1053.
4. Lade, P. V., (1979). (Three-Dimensional Stress - Strain Behaviour and Modelling of Soils), Report, Ruhr University, Bochum.
5. Li, X.S., and Dafalias, Y.F. (2000). "Dilatancy for cohesionless soils." *Geotechnique*, 50(4), 449-460.
6. Li, X. S., (2002). (A Constitutive Platform for Sand Modeling), 15th ASCE Engineering Mechanics Conference, Columbia University, New York.
7. Molenkamp, F., (1980). (Elasto-Plastic Double Hardening Model, MONOT), Report, Delft Geotechnics.
8. Molenkamp, F., (1985). (A Stress - Strain Curve for Both Hardening and Softening), Proceedings of the International Conference on "Numerical Methods in Engineering, NUMETA85", Swansea, p. p. 489 - 496.
9. Molenkamp, F., (1987). (Kinematic Model for Alternating Loading, ALTERNAT), Report, Delft Geotechnics.

10. Nakata, Y., Hyodo, M., Murata, H., and Yasufuku, N. (1998). "Flow Deformation of Sands Subjected to Principal Stress Rotation." Soils and Foundations, 38(2), 115-128.
11. Rowe, P. W., (1962). (The Stress - Dilatancy Relation for Static Equilibrium of an Assembly of Particles in Contact), Proceedings Royal Society, Vol. 269, p. p. 500 - 527.
12. Rowe, P. W., (1971). (Theoretical Meaning and Observed Values of Deformation Parameters for Soil), Proceedings Roscoe Memorial Symposium, Cambridge, p. p. 143 - 194.
13. Vaid, Y.P., and Chern, J.C. (1985). "Cyclic and Monotonic Undrained Response of Saturated Sands." *Advances in the Art of Testing Soils Under Cyclic Loading*, ASCE National Convention, Detroit, 120-147.
14. Yoshimine, M., Ishihara, K. and Vargas, W. (1998). (Effects of Principal Stress Direction and Intermediate Principal Stress on Undrained Shear Behavior of Sand), Soils and Foundations, 38(3): 189-198.
15. Yoshimine, M.,(2002). (Effect of Anisotropy of Loose Sand in Undrained Triaxial Test), Report on Internet.
16. Zienkiewicz, O. C. and Pande, G. N., (1977). (Some Useful Forms of Isotropic Yield Surfaces for Soil and Rock Mechanics), Chapter 5 in "Finite Elements in Geomechanics", edited by G. Gudehus, p. p. 179 - 190.
17. Zienkiewicz, O. C., Chan, A. H. C., Pastor, M. and Shiomi, T., (1987). (Computational Approach to Soil Dynamics), in "Soil Dynamics and Liquefaction", edited by A. S. Cakmak, (Developments in Geotechnical Engineering - 42), p. p. 3 - 13.

ABBREVIATIONS

ASCE = American Society of Civil Engineers.

JSSMFE = Japanese Society of Soil Mechanics and Foundation Engineering.

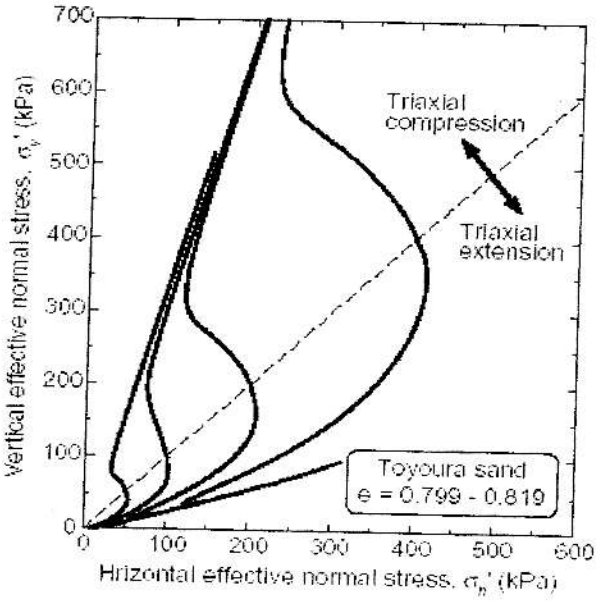

Fig. (1) - Stress path from undrained triaxial compression and extension tests (data from Yoshimine et al., 1998).

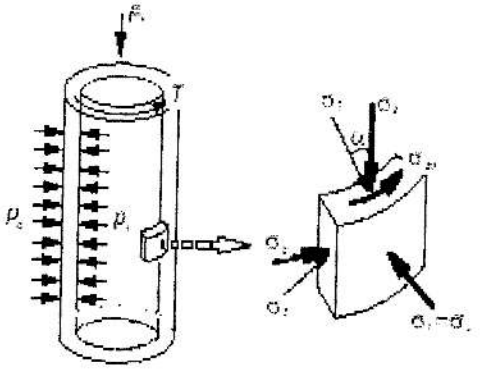

Fig (2) - Rotation of principal stress axes in torsional shear tests (after Yoshimine et al., 1998).

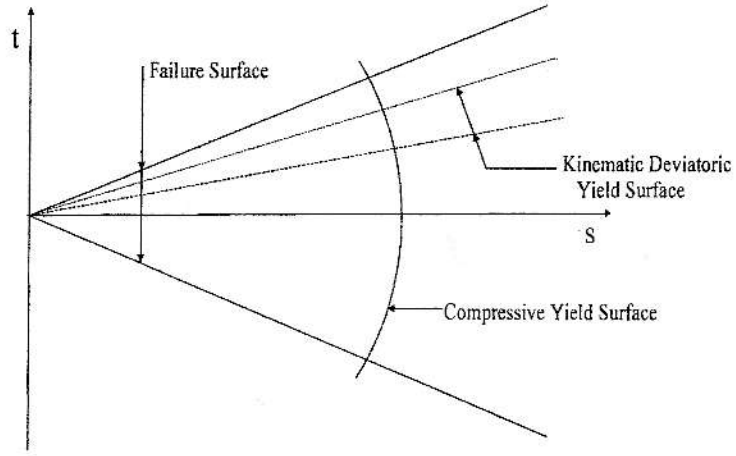

Fig (3) - The yield surfaces of the ALTERNAT model.

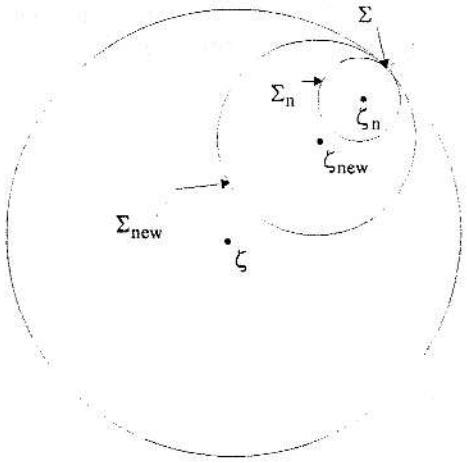

Fig (4) - Definition of the kinematic hardening and the motion of the kinematic yield surfaces.

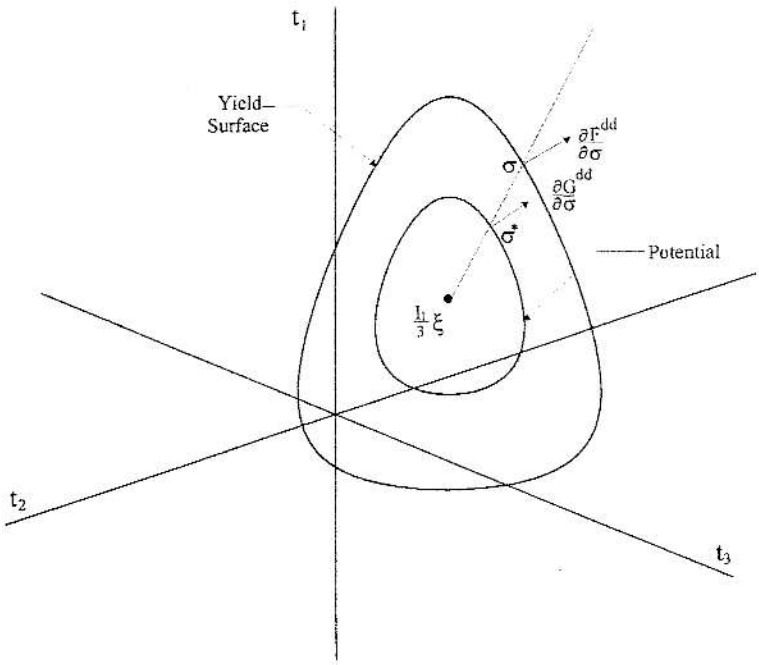

Fig (5) - The yield surface and the plastic potential.

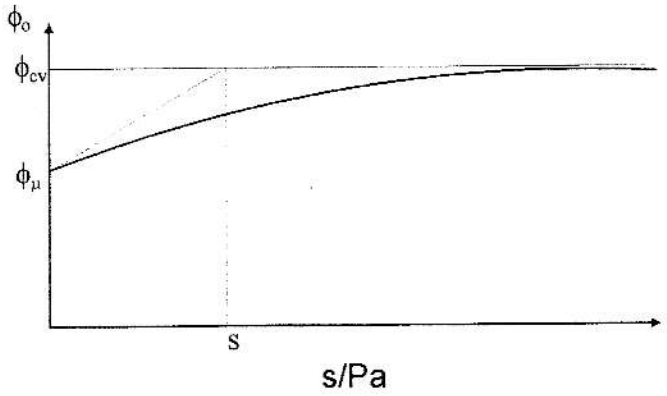

Fig (6) - Definition of the parameters for stress dilatancy.

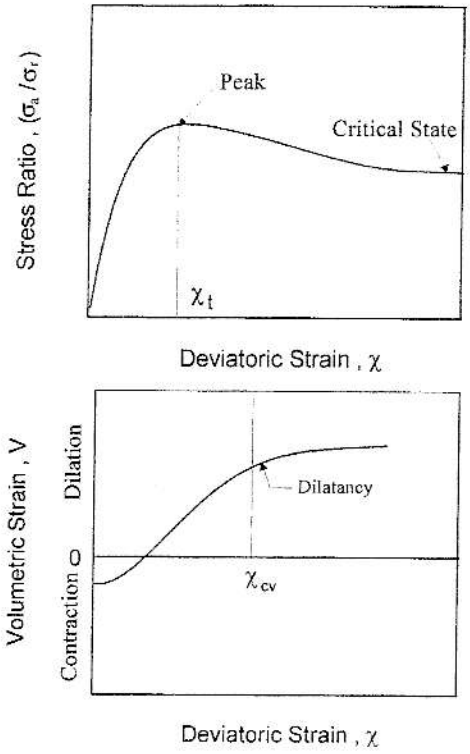

Fig (7) - Definition of the critical state and stress dilatancy.

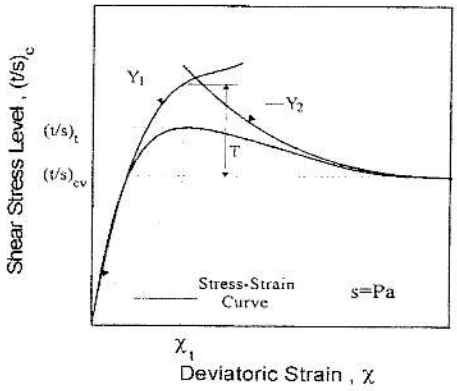

Fig (8) - Approximation for the stress-strain curve in drained triaxial compression test, (after Molenkamp, 1985).

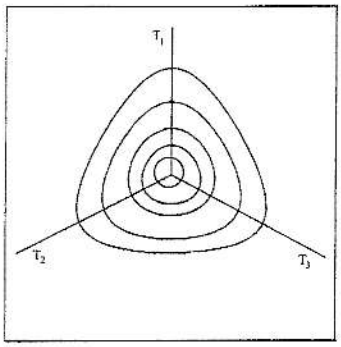

(a)

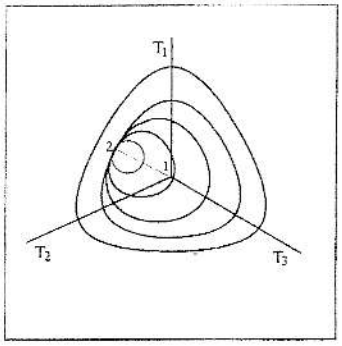

(b)

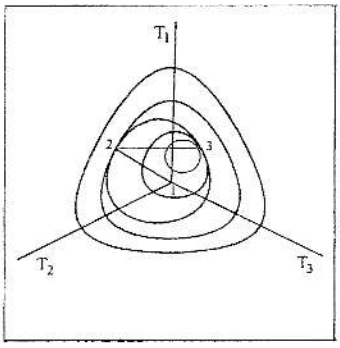

(c)

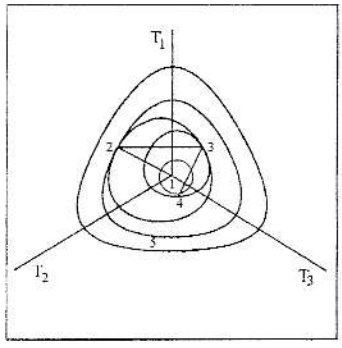

(d)

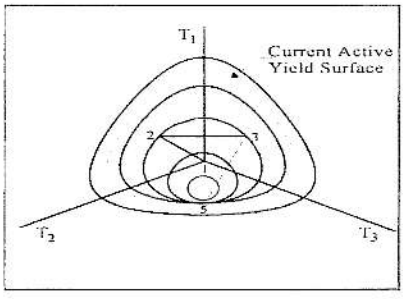

(e)

Note: T_1, T_2 and T_3 are the principal stresses.

Fig (9) - The motion of the yield surfaces during alternating loading, (after Molenkamp, 1987).

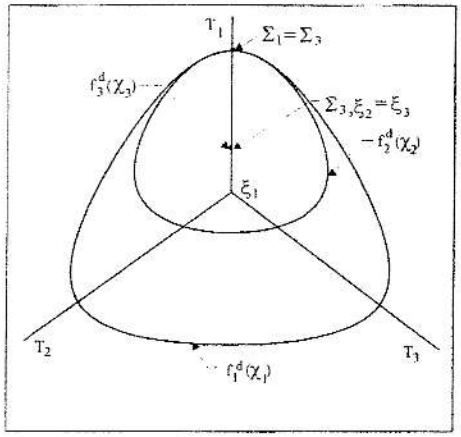

Fig (10) - Definition of the initial state in the pi-plane.

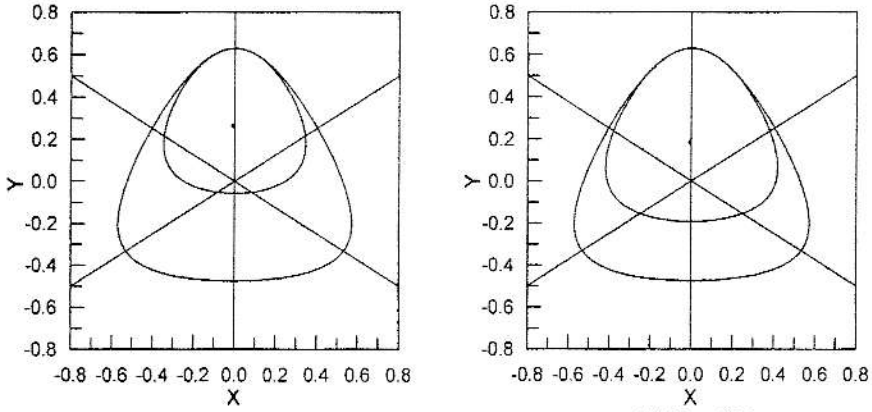

(a) $K_o = 0.6$ (b) $K_o = 0.7$

$$X = (-\sigma_b + \sigma_c) / I_1 * \sqrt{3/2}$$

$$Y = (2 * \sigma_v - \sigma_b - \sigma_c) / I_1 / \sqrt{2}$$

σ_v = vertical stress, σ_b and σ_c are the lateral stresses.

Fig (11) - Kinematic yield surfaces in pi-plane for the initial state at different values of K_o.

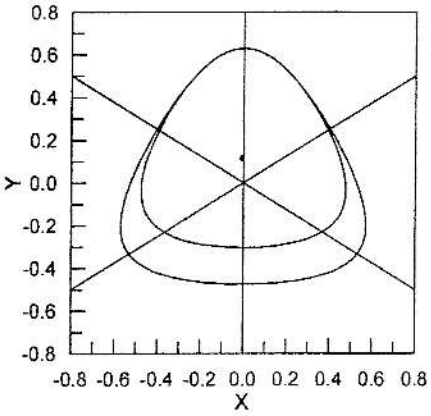

(c) $K_o = 0.8$

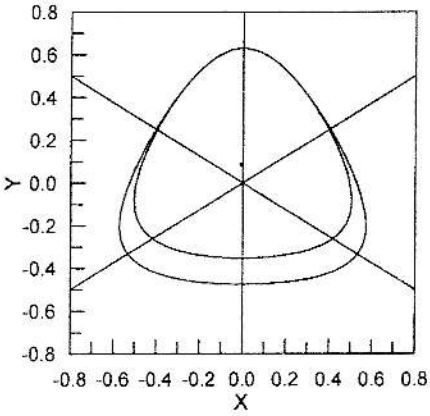

(d) $K_o = 0.85$

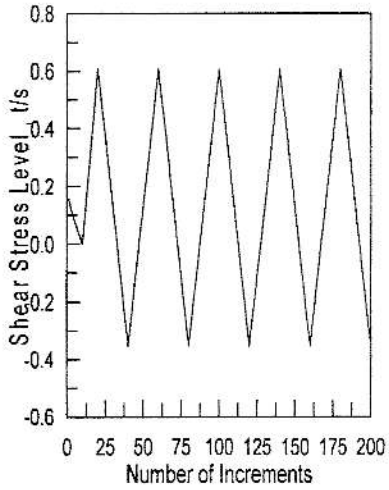

Fig. (12) – Variation of shear stress

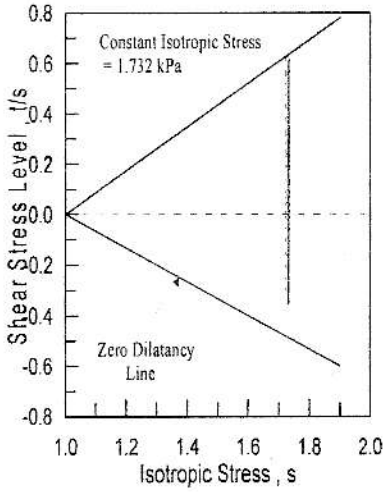

Fig. (13) – Plot of shear stress level

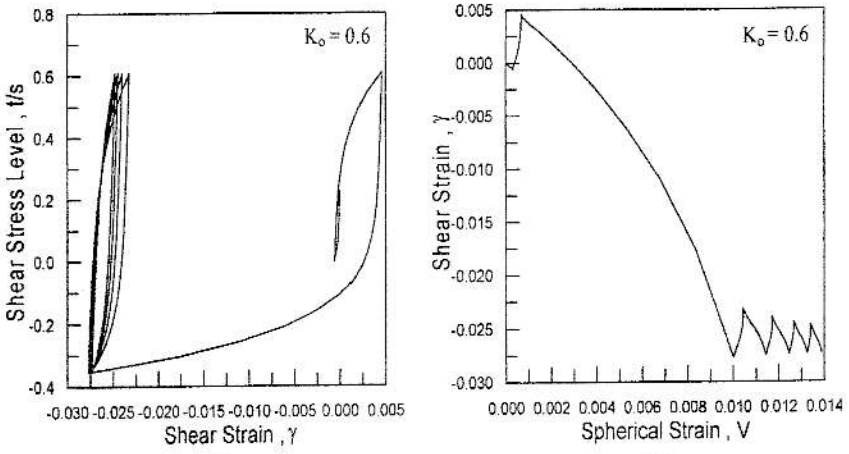

Fig (14) - Numerical prediction of shear and spherical strains, $K_o = 0.6$.

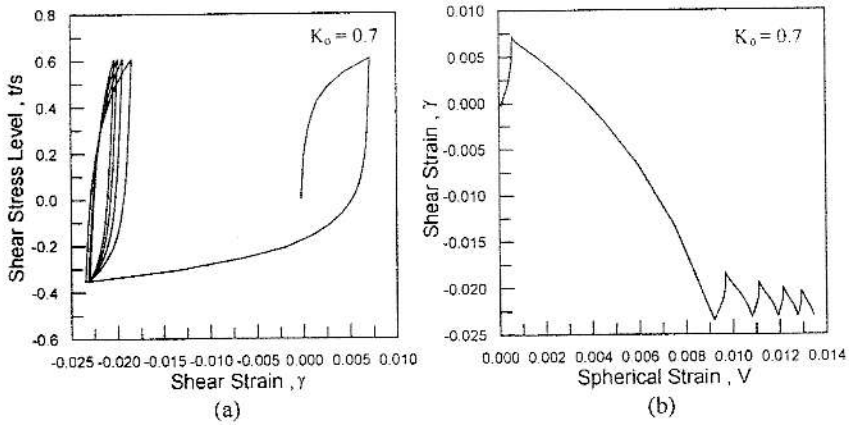

Fig. (15) – Numerical prediction of shear strains, spherical strains and dilatancy ratio, Ko=0.7.

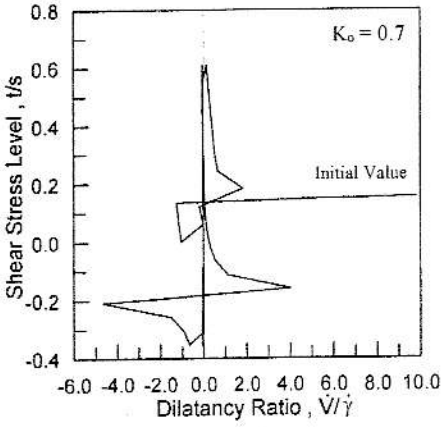

(c)

Fig.(15) – (Continued).

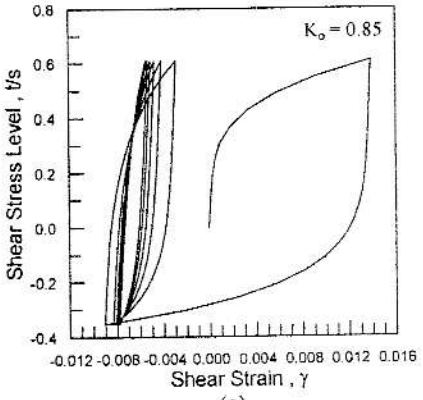

(a)

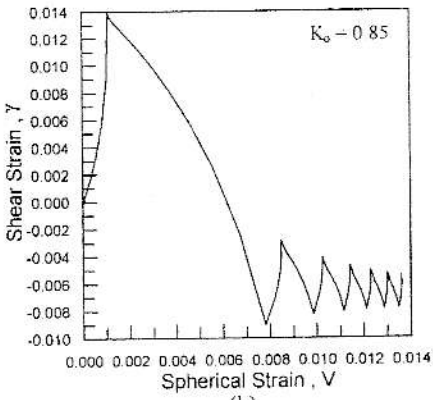

(b)

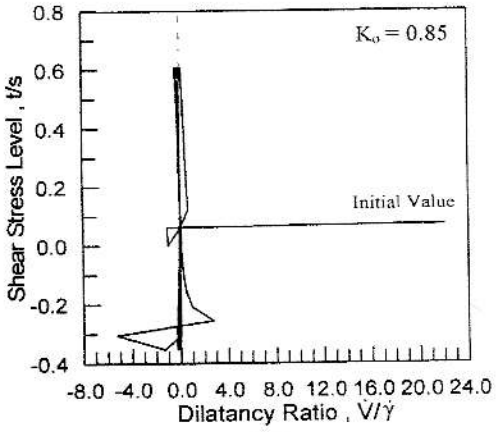

(c)

Fig.(16) Numerical prediction of shear strains, spherical stains and dilatancy ratio, Ko=0.85.

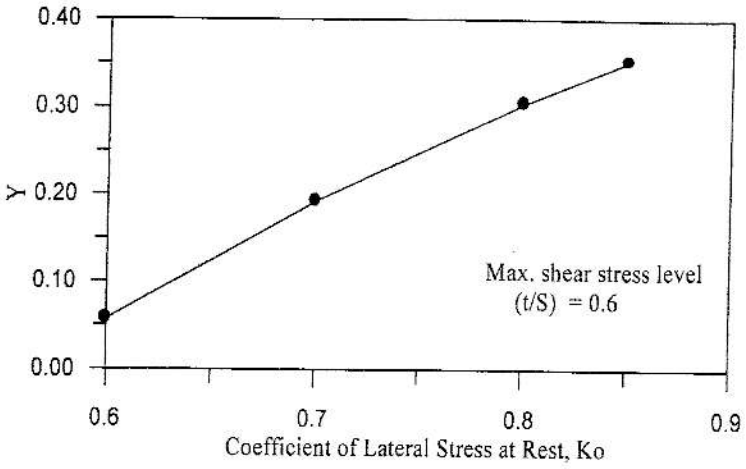

$$Y = (2 * \sigma_v - \sigma_b - \sigma_c) / I_1 / \sqrt{2}$$

Fig. (17) – Effect of coefficient of lateral stress at rest on the invariant, Y.

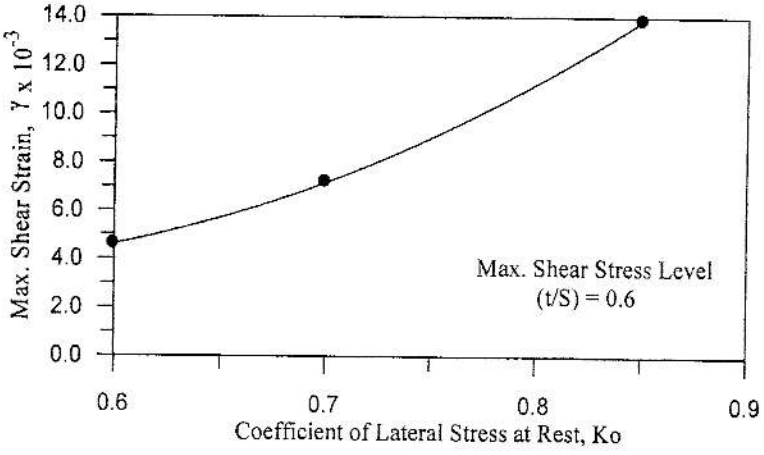

Fig. (18) – Effect of coefficient of lateral stress at rest on the maximum shear strain during cyclic loading..

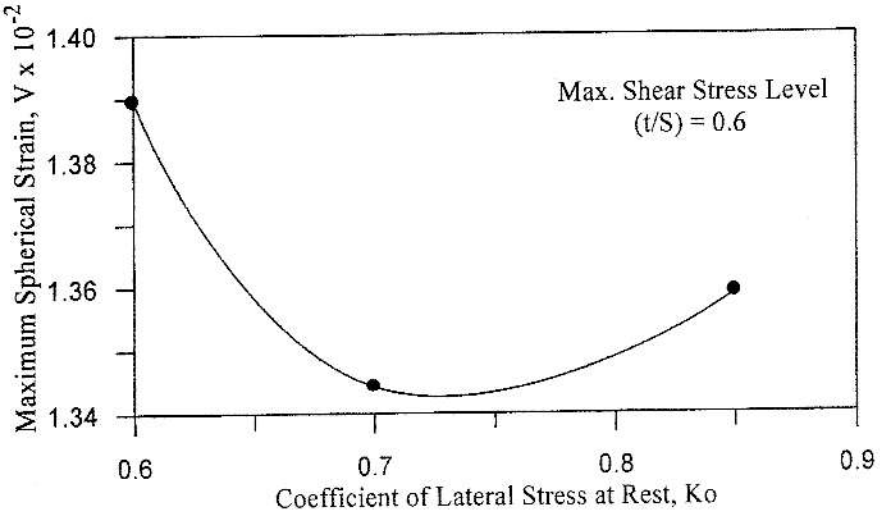

Fig. (19) - Effect of coefficient of lateral stress at rest on the maximum spherical strain during cyclic loading.